Simulations of Merging Neutron Stars and Black Holes as Sources of Gamma-Ray Bursts and Heavy Elements

Maximilian Ruffert

Dept. of Maths & Stats, Univ. of Edinburgh, Scotland EH9 3JZ, U.K.

H.-Thomas Janka

MPI für Astrophysik, Postfach 1523, D–85740 Garching, Germany

Abstract. Hydrodynamic simulations were performed of the dynamical phase of the merging of binary neutron stars (NS+NS) and of neutron star black hole binaries (NS+BH), using a physical nuclear equation of state (Lattimer & Swesty 1991) and taking into account the emission of gravitational waves and neutrinos.

1. Introduction and Summary of Numerics

NS+NS and NS+BH mergers have been suggested as sources of γ-ray bursts at cosmological distances (e.g. Narayan et al 1992) and of r-process nuclei (Eichler et al 1989). These merger events are estimated to occur at rates of the order 10^{-5} per year per galaxy (e.g. Fryer & Woosley 1999).

In order to simulate the merging of two neutron stars and of neutron stars with black holes with the aim to compute neutrino and gravitational-wave emission, the three-dimensional Newtonian equations of hydrodynamics were integrated by the 'Piecewise Parabolic Method'. We took into account the effects of the emission of gravitational waves and the corresponding backreaction on the hydrodynamics. The properties of neutron star matter were described by the equation of state of Lattimer and Swesty (1991). Energy loss and changes of the electron abundance due to the emission of neutrinos were taken into account by an elaborate "neutrino leakage scheme", which is based on a careful evaluation of the lepton number and energy source terms of all neutrino and antineutrino flavors. The simulations were performed with four nested Cartesian grids which allowed for both a good resolution near the central black hole and a large computational volume. In a post-processing step, we evaluated our models for the energy deposition by $\nu\bar{\nu}$ annihilation around the merging objects.

2. Simulations

We have carried out a large number of simulations of neutron star mergings (Ruffert et al 1996, 1997), neutron star collisions (Ruffert & Janka 1998), the post-merging evolution of neutron stars (Ruffert & Janka 1999), and neutron star black hole mergers (Eberl 1998).

Table 1. Results of merger models. Energies are given in units of 1foe = 10^{51} erg.

model	masses ($M_\odot$)	spin	$\Delta M_{\rm d}$ $\left(\frac{M_\odot}{100}\right)$	$t_{\rm sim}$ (ms)	$\langle L_\nu \rangle$ $\left(100\,\frac{\rm foe}{\rm s}\right)$	$a_{\rm BH}$	q_ν %	$q_{\nu\bar{\nu}}$ %	$\dot{E}_{\nu\bar{\nu}}$ $\left(\frac{\rm foe}{\rm s}\right)$	$t_{\rm acc}$ (ms)	E_ν (foe)	$E_{\nu\bar{\nu}}$ (foe)
NS+NS	1.2–1.2	solid	2.0	10	1.5	—	—	1.0	1.4	—	—	—
NS+NS	1.2–1.8	solid	3.8	13	2.0	—	—	1.3	2.6	—	—	—
NS+NS	1.6–1.6	anti	0.01	10	4.0	—	—	1.5	6.0	—	—	—
NS+NS	1.6–1.6	none	0.23	10	5.0	—	—	1.8	9.1	—	—	—
NS+NS	1.6–1.6	solid	2.4	10	3.3	—	—	2.1	7.0	—	—	—
BH+AD	3.0–0.26	solid	—	15	1.2	0.42	1.3	0.4	0.49	68	8	0.03
BH+NS	2.5–1.6	solid	0.2	10	8.0	0.76	3.0	2.8	22.4	40	32	0.9
BH+NS	5.0–1.6	solid	5.6	15	5.0	0.33	2.8	1.8	9.0	56	28	0.5
BH+NS	10.0–1.6	solid	10.0	10	2.5	0.14	2.8	0.9	2.3	82	21	0.2

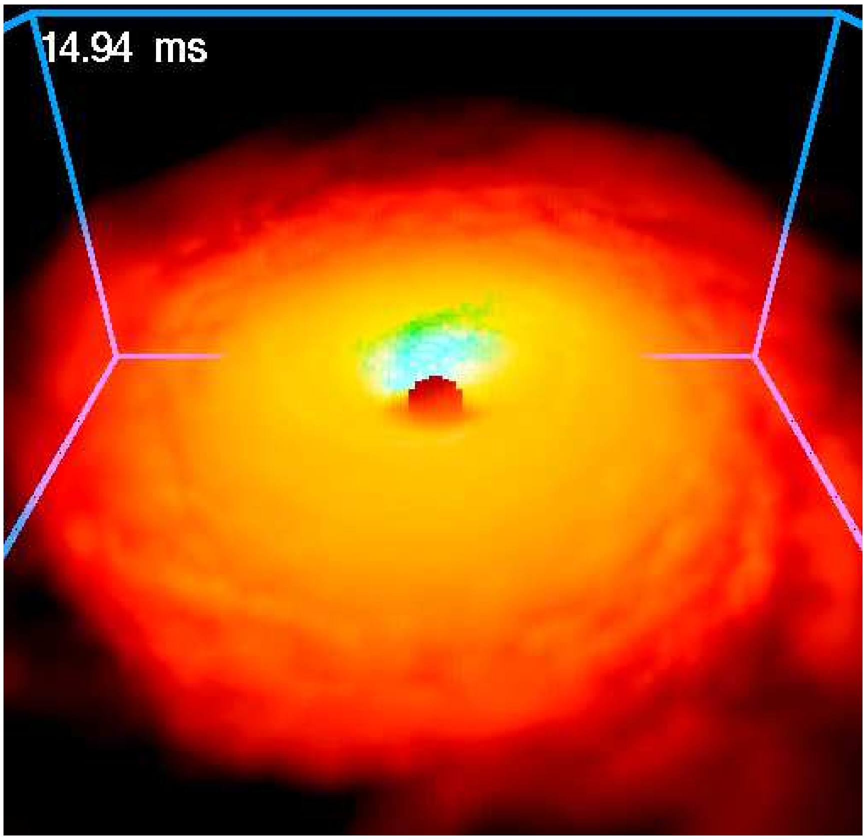

Figure 1. Accretion torus around the black hole which is assumed to form after the merging of two neutron stars. The plot displays the situation about 5 ms after the black hole formation by visualization of the neutrino emission from the hot torus gas. Near the equatorial plane the gas density is very high (maximum density about 10^{12} g/cm^3) whereas a low-density funnel has opened up along the rotation axis.

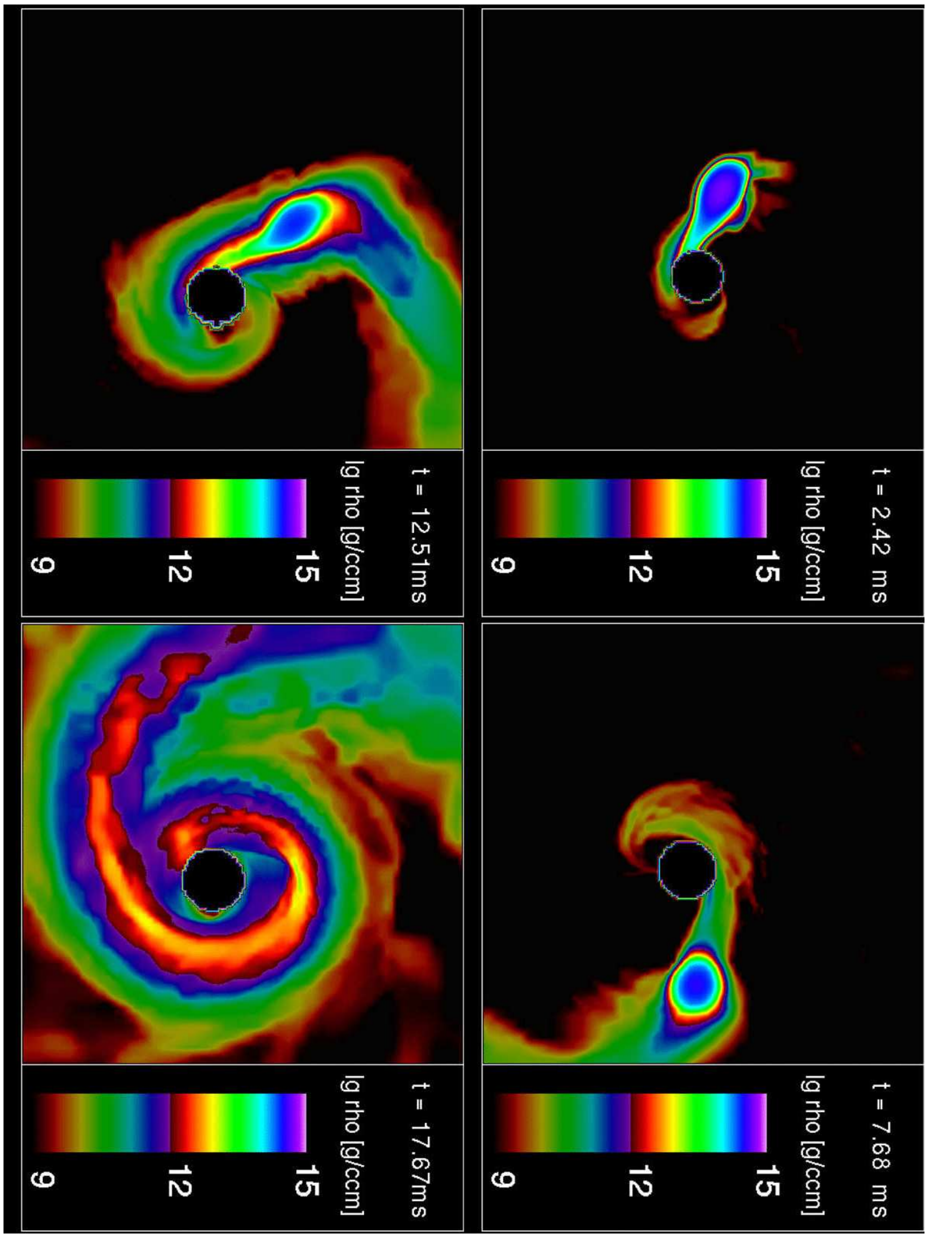

Figure 2. Stages of the merging of a $1.6\,M_{\odot}$ neutron star (baryonic mass) with a $5\,M_{\odot}$ black hole according to a simulation by Eberl (1998). The density in the orbital plane is plotted logarithmically. The neutron star finally gets disrupted after several cycles of approach, mass transfer and subsequent orbit widening.

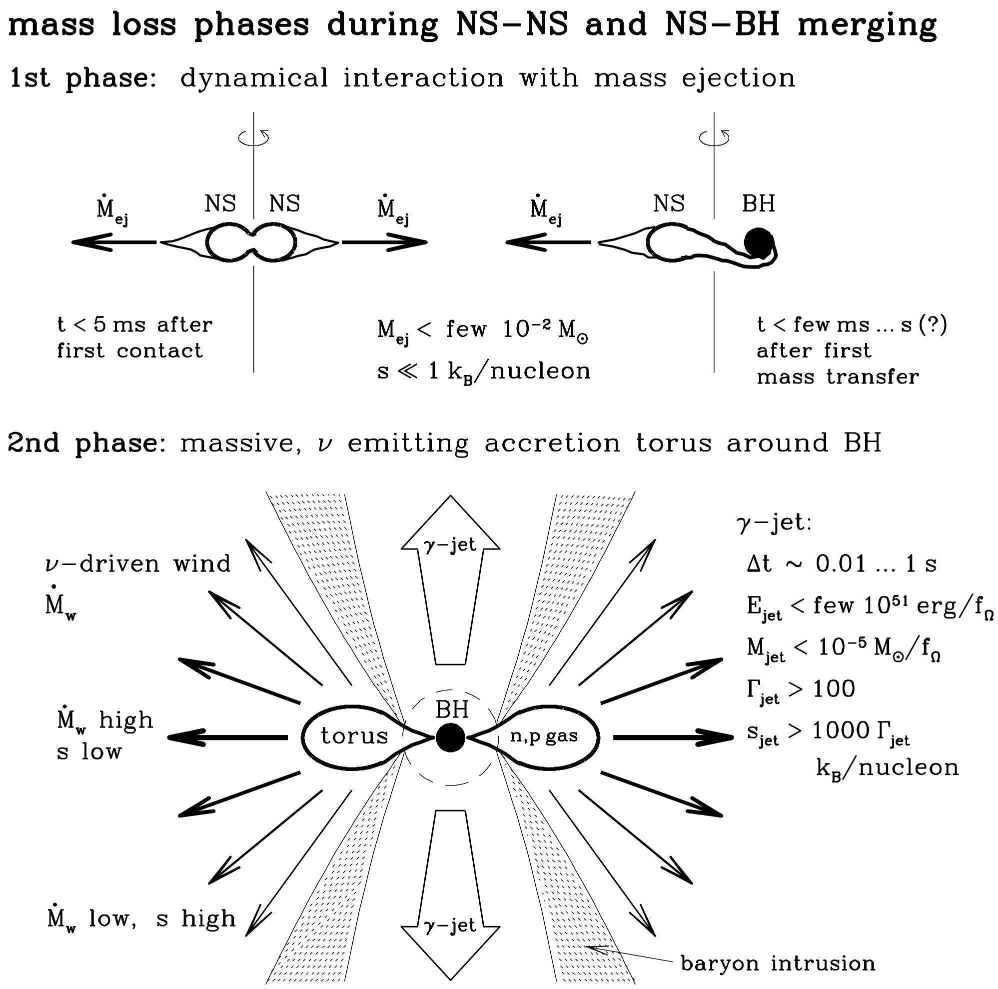

Figure 3. Mass-loss phases during NS+NS and NS+BH merging and during the subsequent evolution of the massive accretion disk that forms around the black hole.

The results of these models with different parameters such as neutron star and/or black hole masses, mass ratios and impact parameters, shed light on the physical conditions accessible during the merger, on the conversion of energy into neutrino emission, on the timescales of mass accretion by the black hole assumed to be formed after neutron star merging, and on the amount of matter dynamically ejected during the merging.

Results for several of our simulations are listed in Table 1. The neutron star and accretion disk (AD) masses are baryonic masses, the spin parameter indicates whether no spin was assumed for the neutron stars ("none"), or the neutron star spin was taken parallel ("solid") or anti-parallel ("anti") to the orbital angular momentum. $\Delta M_{\rm d}$ is the dynamically ejected mass, $t_{\rm sim}$ the time at the end of the simulation, $\langle L_\nu \rangle$ the typical total neutrino luminosity, $a_{\rm BH} = Jc/(GM_{\rm BH}^2)$ the relativistic rotation parameter of the black hole, $q_\nu = L_\nu/(\dot{M}c^2)$

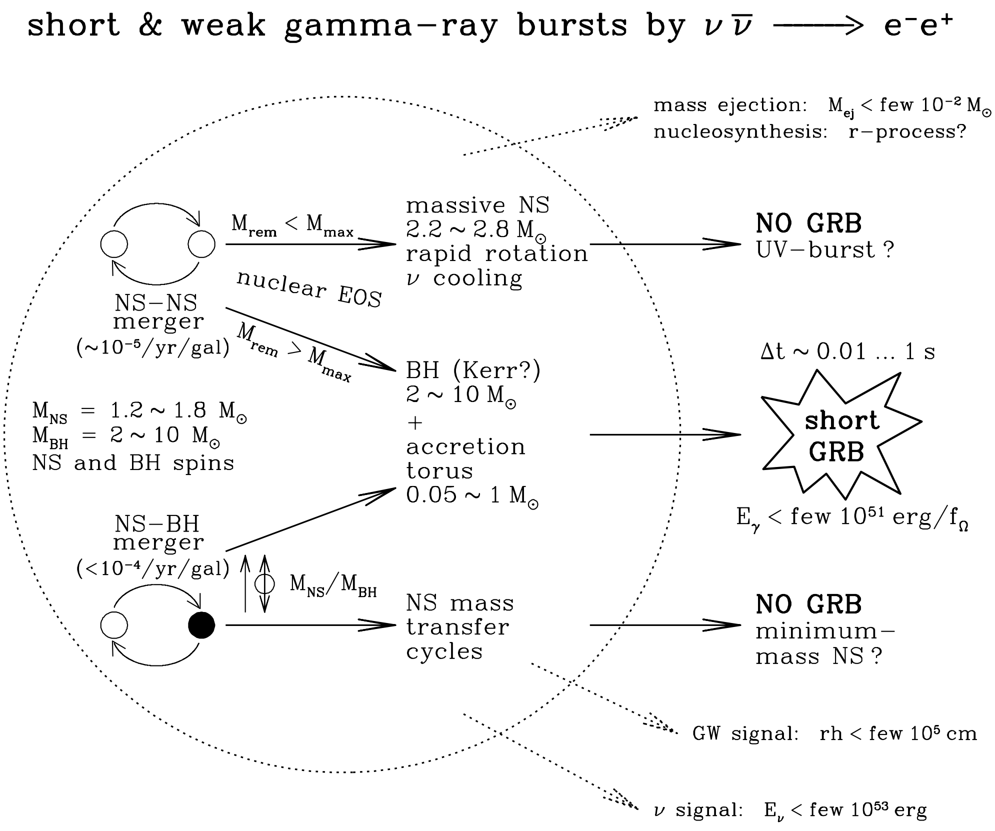

Figure 4. Possible evolution paths from NS+NS and NS+BH mergers to short γ-ray bursts powered by $\nu\bar{\nu}$ annihilation into $e^\pm$ pairs.

the conversion efficiency of rest-mass energy of the gas swallowed by the black hole into ν energy, $q_{\nu\bar{\nu}} = E_{\nu\bar{\nu}}/E_\nu$ the conversion efficiency of ν energy into $e^\pm$ pairs, $\dot{E}_{\nu\bar{\nu}}$ the integral rate of energy deposition by $\nu\bar{\nu}$ annihilation, $t_{\rm acc}$ the estimated duration of the accretion by the black hole, E_ν the energy released in neutrinos during $t_{\rm acc}$, and $E_{\nu\bar{\nu}}$ the corresponding energy converted into $e^\pm$ pairs.

During the merging of two neutron stars, a small amount of matter is ejected (Sect. 3) but the major part forms a very compact remnant of about $2.5\,M_\odot$, surrounded by a cloud of more dilute gas with high angular momentum and a mass of several tenths of a solar mass. The subsequent evolution depends on the stiffness of the finite-temperature nuclear equation of state and the question whether the hot, rapidly spinning remnant is above or below the maximum mass for stable neutron stars. Without a relativistic dynamical investigation the question cannot be decided whether and if, when the merger remnant collapses to a black hole.

If the nuclear equation of state is sufficiently stiff, the merger remnant will remain stable and will cool by neutrino emission over a period of tens of seconds like a massive, newly formed neutron star in a supernova explosion. In this case, neutrino energy deposition in the surface layers of the remnant will drive

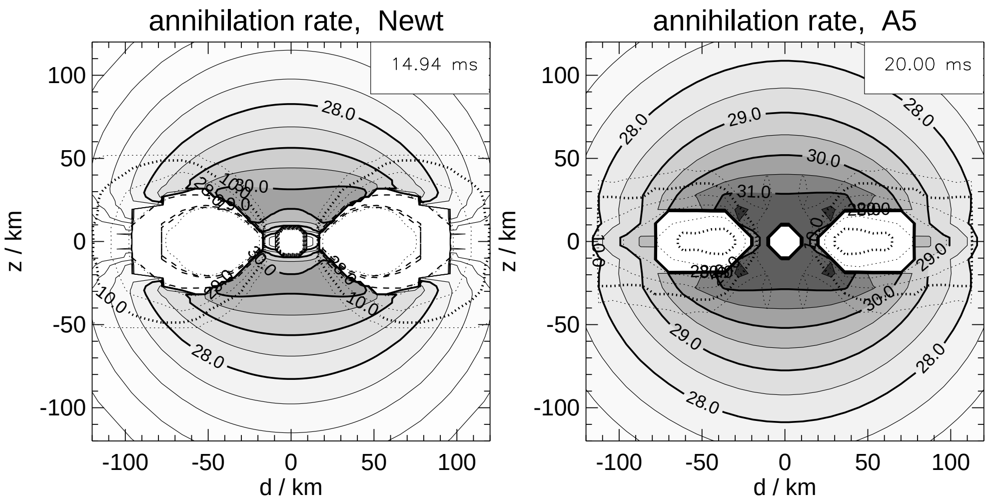

Figure 5. Azimuthally averaged maps of the rate density of energy deposition by $\nu\bar{\nu}$ annihilation into e^+e^- pairs (in erg $\mathrm{cm}^{-3}\mathrm{s}^{-1}$, contours represent logarithms, the levels are spaced in steps of 0.5 dex) in the surroundings of the accreting black hole (white octagonal area at the center) which originates from the merging of two neutron stars with $1.6\,M_\odot$ baryonic mass (left) or of a $1.6\,M_\odot$ neutron star with a $5\,M_\odot$ black hole (right). In the former case the accretion disk (AD) has a mass of $0.26\,M_\odot$ and the total energy deposition rate below a density of $10^{11}\,\mathrm{g\,cm}^{-3}$ is $4.9 \times 10^{50}\,\mathrm{erg\,s}^{-1}$. In the latter case the AD mass is $0.45\,M_\odot$ and the integral energy deposition rate is 15 times higher, $71.6 \times 10^{50}\,\mathrm{erg\,s}^{-1}$. The dotted lines represent isodensity contours of the AD, the dashed lines show the neutrinospheres for the different ν and $\bar{\nu}$ flavors. The time after the start of the simulation is given in the upper right corner.

a baryonic mass outflow (Duncan et al 1986, Paczyński 1990). Although the conditions in this neutrino-driven wind are not far away from those required for an r-processing, hopes could not be confirmed that the wind is the long-sought site for the creation of the r-process elements (Qian & Woosley 1996). Also, the large amount of wind material which is blown off the remnant surface in all directions prevents relativistic expansion. The high mass-loss rates therefore seem to rule out the production of gamma-ray bursts at cosmological distances (Woosley & Baron 1992, Woosley 1993).

The situation is more favorable if the nuclear equation of state is so soft that the merger remnant cannot be supported by pressure and centrifugal forces, but collapses to a black hole only a few milliseconds after its formation. In this case matter with high angular momentum continues orbiting around the black hole until it gets accreted on a timescale determined by the viscous transport of angular momentum. In contrast, because of its low angular momentum the gas near the rotation axis is sucked into the hole within only milliseconds, and a low-density funnel opens up. Figure 1 shows the situation for a simulation where we replaced the central core of the remnant by a vacuum sphere about

9 ms after the two neutron stars had merged (which is 10 ms after the start of the computation). We continued the modelling for another 5 ms using a Newtonian central potential to describe the gravitational influence of the assumed black hole inside the vacuum sphere.

When neutron stars merge with stellar-mass black holes, the neutron star gets torn apart when it comes close to the black hole. For the case of neutron star to black hole mass ratios below a certain critical value, we find that this happens after several mass-transfer cycles, whereas for larger mass ratios the disruption can occur even during the first approach. In all cases, we found that a significant amount of matter (up to more than $0.5\,M_\odot$) ends up in a torus which will evolve on timescales dictated by viscous effects. The torus geometry is characterized by a large asymmetry with the axis being a preferred direction with favorable conditions for the development of highly relativistic outflows with low baryon loading (Mochkovitch et al 1993).

3. Mass Ejection

We find that during the dynamical phase of the merging between about $10^{-4}\,M_\odot$ and several $10^{-2}\,M_\odot$ of cool gas can be ejected (Fig. 3). The exact number depends very sensitively on the assumed neutron star spin(s) and on the masses of the merging binary components (Table 1). This is of potential interest for heavy-element nucleosynthesis (Rosswog et al 1999).

Figure 3 sketches the result that during the dynamical interaction of the binary components (1st phase) low-entropy (dense and cold) matter is ejected from the ends of long spiral arms which are formed in the orbital plane. During the merging the matter is heated by shocks and viscous dissipation, and intense neutrino fluxes are emitted before the gas is accreted into the central black hole. Energy transfer by these neutrinos drives a high-entropy gas outflow ("neutrino wind") off the surface of the accretion disk. At the same time, energy deposition by $\nu\bar{\nu}$ annihilation in the essentially baryon-free funnel around the rotation axis powers relativistically expanding $e^{\pm}\gamma$ jets which can give rise to γ-ray bursts.

4. Neutrino Emission and Implications for Gamma-Ray Bursts

Our simulations confirm suggestions that these events could be the sources of a subclass of short gamma-ray bursts at cosmological distances (Fig. 4). BH+NS mergers yield between 10 and 100 times more energy than NS+NS mergers (Table 1). The annihilation of neutrinos and antineutrinos (Fig. 5) which are emitted from the hot matter that is accreted into the (forming) black hole, yields total energies $E_{\nu\bar{\nu}}$ up to 10^{51} erg in our models. It is therefore enough efficient to explain observable burst luminosities $L_\gamma \sim E_{\nu\bar{\nu}}/(f_\Omega t_\gamma)$ up to several $10^{53}\,\mathrm{erg\,s^{-1}}$ for burst durations $t_\gamma \approx 0.1$–$1\,\mathrm{s}$, if the γ emission is beamed in two moderately focussed jets into a fraction $f_\Omega = 2\delta\Omega/(4\pi) \approx 1/100$—$1/10$ of the sky. Such a modest amount of beaming (jet opening half-angles between about ten and several ten degrees) has to be expected because the dense gas in the equatorial plane of the accreting black hole prevents relativistic expansion of the pair-plasma jets outside a low-density funnel along the system axis. More energy for the burst can be available if Kerr effects of the rotating black hole are taken into account.

The evolution tracks of compact binaries shown in Fig. 4 depend on the neutron star and black hole masses, on the total angular momentum in the system, and on the stiffness of the nuclear equation of state. Energetic relativistic pair-plasma jets can be produced when a hot accretion disk forms around the black hole, because high neutrino fluxes are emitted over a time much longer than the dynamical timescale of the system. This allows for high efficiencies q_ν and $q_{\nu\bar{\nu}}$ and a large total energy conversion by $\nu\bar{\nu} \to e^+e^-$. Gamma-ray bursts from these scenarios are accompanied by the ejection of nucleosynthesis products in considerable amounts, the emission of large numbers of neutrinos with MeV energies, and the production of strong gravitational-wave signals.

Acknowledgments. MR is grateful for support by a PPARC Advanced Fellowship, HTJ acknowledges support by the DFG on grant "SFB 375 für Astro-Teilchenphysik".

References

Duncan, R.C., Shapiro, S.L., Wasserman, I. 1986, ApJ, 309, 141

Eberl, T. 1998, Diploma Thesis, Technical University Munich

Eberl, T., Ruffert, M., Janka, H.-Th., Fryer, C. 1999, in preparation

Eichler, D., Livio, M., Piran, T., Schramm, D.N. 1989, Nature, 340, 126

Fryer, C., Woosley, S.E. 1998, ApJ, 502, L9

Lattimer, J.M., Swesty, F.D. 1991, Nucl. Phys., A535, 331

Mochkovitch, R., Hernanz, M., Isern, J., Martin, X. 1993, Nature, 361, 236

Narayan, R., Paczyński, B., Piran, T. 1992, ApJ, 395, L83

Paczyński B. 1990, ApJ, 363, 218

Qian, Y.-Z., Woosley, S.E. 1996, ApJ, 471, 331

Rosswog, S., *et al.* 1999, A&A, 341, 499

Ruffert, M., Janka, H.-Th., Schäfer, G. 1996, A&A, 311, 532

Ruffert, M., Janka, H.-Th., Takahashi, K., Schäfer, G. 1997, A&A, 319, 122

Ruffert, M., Janka, H.-Th. 1998, A&A, 338, 535

Ruffert, M., Janka, H.-Th. 1999, A&A, 344, 573

Woosley, S.E. 1993, A&ASuppl., 97, 205

Woosley, S.E., Baron, E. 1992, ApJ, 391, 228